arXiv:1903.03315v6 [cs.LG] 9 Jan 2020

Provable Tensor Ring Completion

Huyan Huang[a], Jiani Liu[a], Yipeng Liu[a,1,*], Ce Zhu[a]

[a]*School of Information and Communication Engineering, University of Electronic Science and Technology of China (UESTC), Chengdu, 611731, China.*

Abstract

Tensor completion recovers a multi-dimensional array from a limited number of measurements. Using the recently proposed tensor ring (TR) decomposition, in this paper we show that a d-order tensor of size $n \times \cdots \times n$ and TR rank $[r, \ldots, r]$ can be exactly recovered with high probability by solving a convex optimization program, given $O\left(n^{\lceil d/2 \rceil} r^2 \ln^7\left(n^{\lceil d/2 \rceil}\right)\right)$ samples. The proposed TR incoherence condition under which the result holds is similar to the matrix incoherence condition. The experiments on synthetic data verify the recovery guarantee for TR completion. Moreover, the experiments on real-world data show that our method improves the recovery performance compared with the state-of-the-art methods.

Keywords: Tensor completion, Tensor ring decomposition, Convex optimization, Tensor ring incoherence condition, Nuclear norm minimization

*Corresponding author.

Email addresses: huyanhuang@gmail.com (Huyan Huang), jianiliu@std.uestc.edu.cn (Jiani Liu), yipengliu@uestc.edu.cn (Yipeng Liu), eczhu@uestc.edu.cn (Ce Zhu)

[1]This research is supported by National Natural Science Foundation of China (NSFC, No. 61602091, No. 61571102).

1. Introduction

Tensors are natural representations for multi-dimensional data [1, 2, 3]. In the mathematical discipline of multi-linear algebra, one fundamental problem is how to express a tensor as a sequence of elementary operations acting on other simpler tensors (often interpretable). Any scheme that achieves this goal is called tensor decomposition. Tensor decomposition can capture the interactions between different modes of multi-dimensional data, thus it provides a reasonable and advantageous mathematical framework for formulating and solving problems in a range of applications, such as signal processing [2], machine learning [4], remote sensing [5, 6], computer vision [7], etc.

Tensor completion aims to interpolate the missing entries from partially observed tensors [8]. One major theoretical issue in this field concerns the sampling condition for tensor completion which depends on the algebraic structure of tensor decomposition. For instance, based on CANDECOMP/PARAFAC (CP) decomposition which represents a tensor as a sum of rank-1 tensors [1], the method proposed in [9] can recover a d-order tensor of size $n \times \cdots \times n$ and CP rank r, as long as the number of Gaussian measurements is on the order of $n^{\lceil d/2 \rceil} r$. However, determining CP rank is NP-hard [10] and a low CP rank approximation may involve numerical problems [2]. Based on Tucker (TK) decomposition which factorizes a tensor into a set of matrices and one small core tensor [1], [11] claims that it requires $O\left(n^{d-1} r\right)$ Gaussian measurements to recover a d-order tensor of size $n \times \cdots \times n$ and TK rank $[r, \ldots, r]$. Moreover, the number of samples required to recover a tensor by TK decomposition is further reduced to $O\left(n^{\lceil d/2 \rceil} r^{\lfloor d/2 \rfloor}\right)$ via a balance unfolding scheme [9]. Based on another widely used factorization namely tensor

singular value decomposition (t-SVD) [12], the authors of [13] show that a d-order tensor of size $n \times \cdots \times n$ and tubal rank r can be exactly recovered, so long as $O\left(n^{d-1} r \ln\left(n^{d-1}\right)\right)$ entries are sampled under random sampling. Methods based on tensor train (TT) decomposition and hierarchical Tucker (HT) decomposition under random sampling can refer to [14] and [15].

The recently proposed tensor ring (TR) decomposition represents a high-order tensor as several cyclically contracted 3-order tensors [16, 17], which is a linear combination of TT. The first TR decomposition based method is proposed in [18], in which the completion model is formulated as a data fitting problem for the given partial observations. The algorithm optimizes each latent TR factor alternately. However, this method suffers from expensive time cost and overfitting problem when a smaller number of samples are available, and its performance highly rests on the choice of TR rank. Subsequently, a gradient descent method for TR completion is proposed in [19], where all TR factors are simultaneously optimized in one iteration. This method reduces computational cost but still requires a pre-defined TR rank. By exploiting the low rank structure of the TR latent space, a nuclear norm regularization model is propounded to alleviate the burden of TR rank selection [20], which greatly reduces the computational cost. In [21], a TR nuclear norm minimization model with tensor circular unfolding scheme is proposed for tensor completion. This method does not require a pre-defined TR rank and achieves better performance than previous TR decomposition based methods.

However, existing TR decomposition based completion methods do not have theoretical guarantee. In this paper, by leveraging the McDiarmid in-

equality, we prove that most tensors satisfy TR incoherence property if we constrain the mode-2 fibers of TR factors to be incoherent. Using an i-shifting l-matricization scheme [22], we propose a TR nuclear norm minimization model for tensor completion with random sampling. We show that the proposed method can recover a d-order tensor of size $n \times \cdots \times n$ and TR rank $[r, \ldots, r]$ with high probability under the TR incoherence condition, given $O\left(n^{\lceil d/2 \rceil} r^2 \ln^7\left(n^{\lceil d/2 \rceil}\right)\right)$ samples. The proposed theory and the effectiveness of the algorithm are confirmed by experiments on synthetic data and real-world data.

The rest of this paper is organized as follows. Section 2 provides basic notations and preliminaries of TR decomposition. In Section 3, we propose a weighted sum of nuclear norm model for tensor completion with recovery guarantee under random sampling. The corresponding proof is in Section 4. Section 5 exhibits the results of numerical experiments. Finally, we conclude our work in section 6.

2. Notations and Preliminaries

2.1. Notations

This subsection introduces some basic notations of tensor and TR decomposition. For example, a scalar, a vector, a matrix and a tensor are denoted by a normal letter x, a boldface lowercase letter $\mathbf{x}$, a boldface uppercase letter $\mathbf{X}$ and a calligraphic letter $\mathcal{X}$, respectively. Specifically, a d-order tensor of size $n_1 \times \cdots \times n_d$ is denoted as $\mathcal{X} \in \mathbb{R}^{n_1 \times \cdots \times n_d}$, where n_i is the dimensional size corresponding to mode-i, $i = 1, \ldots, d$. The $(j_1 \cdots j_d)$-th entry of $\mathcal{X}$ is denoted as $x_{j_1 \cdots j_d}$. A mode-i fiber of $\mathcal{X}$ is represented as $\mathbf{x}_{j_1 \cdots j_{i-1} j_{i+1} \cdots j_d}$, and

a mode-i slice is denoted as $\mathcal{X}_{\cdots j_i \cdots}$.

We use $\mathbf{E}$ to denote an identity matrix, $\mathscr{I}(\cdot)$ to denote an identity operator and $\|\mathbf{X}\|_2$ to denote the spectral norm of $\mathbf{X}$. The inner product of $\mathcal{X}$ and $\mathcal{Y}$ is defined as $\langle \mathcal{X}, \mathcal{Y} \rangle = \sum_{j_1=1}^{n_1} \cdots \sum_{j_d=1}^{n_d} x_{j_1 \cdots j_d} y_{j_1 \cdots j_d}$. The Frobenius norm of $\mathcal{X}$ is defined as $\|\mathcal{X}\|_{\mathrm{F}} = \sqrt{\langle \mathcal{X}, \mathcal{X} \rangle}$. The Kronecker product and Hadamard product are expressed as $\otimes$ and $\circledast$, respectively. A zero tensor is expressed as $\mathcal{O}$. The $O(\cdot)$ is an asymptotic notation. For example, $O(m)$ means a quantity bounded in magnitude by Cm for a constant $C > 0$.

2.2. Tensor Ring Decomposition

Let $\{\mathcal{G}\} = \left\{\mathcal{G}^{(1)}, \ldots, \mathcal{G}^{(d)}\right\}$, $\mathcal{G}^{(i)} \in \mathbb{R}^{r_i \times n_i \times r_{i+1}}$ denote the normalized factors of TR decomposition on the second dimension and $\left\{\mathbf{\Sigma}^{(1)}, \ldots, \mathbf{\Sigma}^{(d)}\right\}$, $\mathbf{\Sigma}^{(i)} \in \mathbb{R}^{r_{i-1} \times r_i}$ denote the TR singular value matrices. The representation of TR decomposition is $x_{j_1 \cdots j_d} = \mathrm{tr}\left(\mathbf{\Sigma}^{(1)} \mathbf{G}_{j_1}^{(1)} \cdots \mathbf{\Sigma}^{(d)} \mathbf{G}_{j_d}^{(d)}\right)$, where $\mathbf{G}_{j_i}^{(i)}$ is the j_i-th mode-2 slice of $\mathcal{G}^{(i)}$ and $\mathrm{tr}(\cdot)$ is the trace function. Another representation of TR decomposition is $\mathcal{X} = \sum_{t_1=1}^{r_1} \cdots \sum_{t_d=1}^{r_d} \widetilde{\mathbf{g}}_{t_1 t_2}^{(1)} \circ \cdots \circ \widetilde{\mathbf{g}}_{t_d t_1}^{(d)}$, where $\widetilde{\mathbf{g}}_{t_i t_{i+1}}^{(i)} = \sigma_{t_i}^{(i)} \mathbf{g}_{t_i t_{i+1}}^{(i)}$, $\mathbf{g}_{t_i t_{i+1}}^{(i)}$ is the (t_i, t_{i+1})-th mode-2 fiber of $\mathcal{G}^{(i)}$ and $\circ$ denotes the outer product.

Let $\mathbf{X}_{\{i,l\}}$ denote the i-shifting l-matricization of $\mathcal{X}$, which permutes the tensor with order $[i, \ldots, d, 1, \ldots, i-1]$ and performs matricization along first l modes. The indices of $\left(\mathbf{X}_{\{i,l\}}\right)_{pq}$ are

$$p = 1 + \sum_{k=i}^{i+l-1} (j_k - 1) \prod_{m=i}^{k-1} n_m, \; q = 1 + \sum_{k=i+l}^{i-1} (j_k - 1) \prod_{m=i+l}^{k-1} n_m.$$

We use $\overline{\otimes}$ to denote the TR contraction which contracts several TR factors

into a new one. The formulation of TR contraction is

$$\left(\overline{\otimes}_{i=a}^{b}\mathcal{G}^{(i)}\right)_{t_a:t_{b+1}} = \sum_{t_{a+1}=1}^{r_a}\cdots\sum_{t_b=1}^{r_b}\mathbf{g}^{(a)}_{t_a t_{a+1}}\otimes\cdots\otimes\mathbf{g}^{(b)}_{t_b t_{b+1}},$$

where $\overline{\otimes}_{i=a}^{b}\mathcal{G}^{(i)} \in \mathbb{R}^{r_a\times\left(\prod_{i=a}^{b} n_i\right)\times r_{b+1}}$.

3. Main Result

In this section, we consider the TR completion with random sampling. The states of TR are categorized into three types: subcritical, critical and supercritical [17]. We suppose the TR rank is $[r_1,\ldots,r_d]$, the subcritical (supercritical) state requires $r_i r_{i+1} \leq n_i$ ($r_i r_{i+1} \geq n_i$), $\forall i = 1,\ldots,d$, where at least one inequality is strict, and critical state requires $r_i r_{i+1} = n_i$, $\forall i = 1,\ldots,d$. We focus on a study of a (sub)critical TR since a supercritical TR can be reduced to (sub)critical by a surjective birational map [17]. Thereafter a TR means a (sub)critical TR wherever it appears.

We use Ω to denote the set of indices of observations. Denotation $\mathscr{P}_\Omega$ is the orthogonal projection onto Ω. We propose the following convex model for tensor completion using i-shifting l-matricization:

$$\min_{\mathcal{X}} \sum_{i=1}^{\lceil d/2\rceil} w_i\left\|\mathbf{X}_{\{i,l\}}\right\|_*, \text{ s. t. } \mathscr{P}_\Omega\left(\mathcal{X}\right) = \mathscr{P}_\Omega\left(\mathcal{T}\right). \tag{1}$$

It is unlikely that a method can be guaranteed to successfully recover a tensor without the assumption of the TR factors. For instance, if tensor $\mathcal{T}\in\mathbb{R}^{n_1\times\cdots\times n_d}$ consists of the outer product of d standard basis vectors i. e., $\mathcal{T} = \mathbf{e}_{j_1}\circ\cdots\circ\mathbf{e}_{j_d}$, in consequence $\mathcal{T}$ can not be recovered without a priori

knowledge of TR factors if entry $t_{j_1 \cdots j_d}$ is not sampled. To make the recovery feasible, the TR factors are required to be not spiky. We characterize this property as the following strong TR incoherence condition, in which the mode-2 fibers of TR factors play a role of singular vectors (thereby we call them TR singular tensors).

Lemma 1 (Strong TR incoherence condition)**.** *The tensor* $\mathcal{T} \in \mathbb{R}^{n_1 \times \cdots \times n_d}$ *obeys the TR strong incoherence property with parameter* $\boldsymbol{\mu} = [\mu_1, \ldots, \mu_d]$, $\boldsymbol{\mu} \succ \mathbf{0}$ *if for any* $i \in \{1, \ldots, d\}$,

$$|\langle \mathcal{G}^{(i)}_{:j_i:}, \mathcal{G}^{(i)}_{:j_i':} \rangle - \frac{r_i r_{i+1}}{n_i} 1_{j_i = j_i'}| \leq \frac{\mu_i \sqrt{r_i r_{i+1}}}{n_i}, \tag{2}$$

provided that the TR rank is $[r_1, \ldots, r_d]$.

Lemma 1 shows that almost all tensors satisfy the strong TR incoherence property with $\mu_i = O\left(\mu_{B_i} \sqrt{\ln(n_i)}\right)$ if they obey the size property $\max\left\{\mathcal{G}^{(i)}\right\} \leq \sqrt{\mu_{B_i}/n_i}$ with $\mu_{B_i} = O(1)$. This union bound means the TR singular tensors $\left\{\mathbf{g}^{(i)}_{11}, \ldots, \mathbf{g}^{(i)}_{r_i r_{i+1}}\right\}$ are incoherent and there exist small values μ_i that can satisfy the strong TR incoherence property. With the only assumption about the small values of TR singular tensors, this model can generate a generic tensor with uniformly bounded TR factors, which leads to the following result.

Lemma 2. *Let* $\mathcal{T} \in \mathbb{R}^{n_1 \times \cdots \times n_d}$ *be a fixed tensor of TR rank* $[r_1, \ldots, r_d]$ *obeying the strong TR incoherence property with parameter* $\boldsymbol{\mu}$*, then the singular tensors of* $\mathbf{X}_{\{i,l\}}$ *are* $\mathcal{U}^{\{k,l\}} = \prod_{i=k+1}^{k+l-1} r_i^{-1} \overline{\otimes}_{i=k}^{k+l-1} \mathcal{G}^{(i)}$ *and* $\mathcal{V}^{\{k+l,d-l\}} =$

$\prod_{i=k+l+1}^{k-1} r_i^{-1} \overline{\otimes}_{i=k+l}^{k-1} \mathcal{G}^{(i)}$, *and inequalities*

$$\begin{cases} |\langle \mathcal{U}_{:\bar{i}:}^{\{k,l\}}, \mathcal{U}_{:\bar{j}:}^{\{k,l\}} \rangle - \dfrac{r_k r_{k+l}}{\prod_{i=k}^{k+l-1} n_i} 1_{\bar{i}=\bar{j}}| \leq \dfrac{\mu'_{1kl}\sqrt{r_k r_{k+l}}}{\prod_{i=k}^{k+l-1} n_i} \\ |\langle \mathcal{V}_{:\bar{i}:}^{\{k+l,d-l\}}, \mathcal{V}_{:\bar{j}:}^{\{k+l,d-l\}} \rangle - \dfrac{r_k r_{k+l}}{\prod_{i=k+l}^{k-1} n_i} 1_{\bar{i}=\bar{j}}| \leq \dfrac{\mu'_{2kl}\sqrt{r_k r_{k+l}}}{\prod_{i=k+l}^{k-1} n_i} \\ |\langle \mathcal{U}_{:\bar{i}:}^{\{k,l\}}, \mathcal{V}_{:\bar{j}:}^{\{k+l,d-l\}} \rangle| \leq \dfrac{\mu''\sqrt{r_k r_{k+l}}}{\sqrt{\prod_{i=1}^{d} n_i}} \end{cases}$$

holds with probabilities at least $1 - \prod_{i=k}^{k+l-1} n_i^{-3}$, $1 - \prod_{i=k+l}^{k-1} n_i^{-3}$ *and* $1 - e^{-\frac{1}{2}\prod_{i=1}^{d} n_i}$, *respectively, where*

$$\begin{cases} \mu'_{1kl} = O\left(\prod_{i=k}^{k+l-1} \mu_{B_i} \sqrt{\sum_{i=k}^{k+l-1} \ln n_i}\right), \ \mu'_{2kl} = O\left(\prod_{i=k+l}^{k-1} \mu_{B_i} \sqrt{\sum_{i=k+l}^{k-1} \ln n_i}\right) \\ \mu'' = \prod_{i=1}^{d} \mu_{B_i} \end{cases}. \tag{3}$$

Lemma 2 shows that any TR unfolding $\mathbf{X}_{\{i,l\}}$ obeys the strong matrix incoherence condition if the TR is strong incoherent. Note that [21] states that a TR unfolding obeys $\operatorname{rank}\left(\mathbf{X}_{\{i,l\}}\right) \leq r_i r_{i+l}$. We emphasize this inequality becomes equality under specific conditions. We find $\operatorname{rank}\left(\mathbf{X}_{\{i,l\}}\right)$ satisfies the equality if mode-1 and mode-3 slices are linearly independent with $l > 1$ or mode-2 fibers are linearly independent with $l = 1$. The Lemma 2 will not be violated if we assume all mode-2 fibers are linearly independent which leads to the upper bound $\max_i \operatorname{rank}\left(\mathbf{X}_{\{i,l\}}\right) = r_i r_{i+l}$.

Now we state our main result.

Theorem 1 (Tensor ring completion)**.** *Under the hypothesis of Lemma 1,*

supposing m entries of $\mathcal{T}$ are observed with locations sampled uniformly at random and defining $\overline{n}_{il} := \max\left\{\prod_{k=i}^{i+l-1} n_k, \prod_{k=i+l}^{i-1} n_k\right\}$. Then there is a numerical constant C such that if

$$m \geq C \max_i \mu_{il}^2 \overline{n}_{il} r_i r_{i+l} \ln^6\left(\overline{n}_{il}\right), \tag{4}$$

$\mathcal{X}$ is the unique solution to (1) with probability at least $1 - \max_i \overline{n}_{il}^{-3}$, where μ_{il} is the maximal value of (3).

A conclusion that can be drawn directly from (3) and (4) is that on the order of $\overline{n}_{il} r_i r_{i+l} \ln^7\left(\overline{n}_{il}\right)$ samples are needed to recover $\mathcal{T}$. The bound can be improved with a suitable l since a (almost) square matrix leads to lower sample complexity for completion.

As a special case, the TR unfolding can be (nearly) squared by setting $l = \lceil d/2 \rceil$ (since $\overline{n}_{i\lceil d/2 \rceil} = \inf_l \overline{n}_{il}$) if n_i, $i = 1, \ldots, d$ are on a same or similar order of magnitude. In this case, the tensor can be recovered with a minimal number of samples theoretically.

4. Architecture of the Proof

Before we prove Theorem 1, we define $\mathcal{R} \triangleq \mathscr{R}\left(\{\mathcal{G}\}\right) \prod_{i=1}^{d} r_i^{-1} \sum_{i=1}^{\lceil d/2 \rceil} w_i r_i r_{i+l}$ and $\mathscr{A}_{il}^*\left(\cdot\right)$ as the tensorization operator, which is the inverse operator of $\{i, l\}$ unfolding. The following conditions are important for the proof of the main theorem (see Appendix Appendix C for details).

Lemma 3 (Dual certificate of tensor ring completion)**.** *Supposing m satisfies*

(4), then $\mathcal{X} \in \mathbb{R}^{n_1 \times \cdots \times n_d}$ *is the unique minimizer to (1) if*

$$\|\mathscr{P}_{T_{il}}\mathscr{P}_{\Omega_{il}}\mathscr{P}_{T_{il}} - m\prod_{i=1}^{d} n_i^{-1}\mathscr{P}_{T_{il}}\|_2 \leq \frac{m}{2}\prod_{i=1}^{d} n_i^{-1},\ i = 1, \ldots, \lceil d/2 \rceil \quad (5)$$

and there exists $\mathcal{Y}$ *such that*

$$\begin{cases} \|\mathscr{P}_{T_{il}}\left(\mathbf{Y}_{\{i,l\}}\right) - \mathcal{U}_{(2)'}^{\{i,l\}}\mathcal{V}_{(2)}^{\{i+l,d-l\}^{\mathrm{T}}}\|_{\mathrm{F}} \leq \frac{1}{2}\prod_{i=1}^{d} n_i^{-1} \\ \|\mathscr{P}_{T_{il}^{\perp}}\left(\mathbf{Y}_{\{i,l\}}\right)\|_2 \leq \frac{1}{2} \end{cases}, \ i = 1, \ldots, \lceil d/2 \rceil. \quad (6)$$

Proof. *The key idea to prove Theorem 1 is to illustrate that* $\sum_{i=1}^{\lceil d/2 \rceil} w_i\|\mathbf{X}_{\{i,l\}} + \Delta_{\{i,l\}}\|_* > \sum_{i=1}^{\lceil d/2 \rceil} w_i\|\mathbf{X}_{\{i,l\}}\|_*$ *for any feasible perturbation* $\Delta \neq \mathcal{O}$ *supported*

in $\Omega^{\perp}$*. We deduce it like follows*

$$
\begin{aligned}
&\sum_{i=1}^{\lceil d/2\rceil} w_i\|\mathbf{X}_{\{i,l\}}+\mathbf{\Delta}_{\{i,l\}}\|_*-\sum_{i=1}^{\lceil d/2\rceil} w_i\|\mathbf{X}_{\{i,l\}}\|_* \\
\geq&\langle\mathcal{R}+\sum_{i=1}^{\lceil d/2\rceil} w_i\mathscr{A}_{il}^*\left(\mathbf{W}_{\{i,l\}}\right),\Delta\rangle \\
=&\sum_{i=1}^{\lceil d/2\rceil} w_i\|\mathscr{P}_{T_{il}^{\perp}}\left(\mathbf{\Delta}_{\{i,l\}}\right)\|_*+\langle\mathcal{R}-\mathcal{Y},\Delta\rangle \\
=&\sum_{i=1}^{\lceil d/2\rceil} w_i\|\mathscr{P}_{T_{il}^{\perp}}\left(\mathbf{\Delta}_{\{i,l\}}\right)\|_*+\sum_{i=1}^{\lceil d/2\rceil} w_i\langle\mathbf{R}_{\{i,l\}}-\mathscr{P}_{T_{il}}\left(\mathbf{Y}_{\{i,l\}}\right),\mathscr{P}_{T_{il}}\left(\mathbf{\Delta}_{\{i,l\}}\right)\rangle- \\
&\sum_{i=1}^{\lceil d/2\rceil} w_i\langle\mathscr{P}_{T_{il}^{\perp}}\left(\mathbf{Y}_{\{i,l\}}\right),\mathscr{P}_{T_{il}^{\perp}}\left(\mathbf{\Delta}_{\{i,l\}}\right)\rangle \\
\geq&\sum_{i=1}^{\lceil d/2\rceil}\frac{w_i}{2}\left(\|\mathscr{P}_{T_{il}^{\perp}}\left(\mathbf{\Delta}_{\{i,l\}}\right)\|_*-\prod_{i=1}^{d} n_i^{-1}\|\mathscr{P}_{T_{il}}\left(\mathbf{\Delta}_{\{i,l\}}\right)\|_{\mathrm{F}}\right) \\
\geq&0.
\end{aligned}
$$

The first inequality comes from the convexity of nuclear norm and second-order Taylor's expansion. Since $\mathscr{P}_{T_{il}}\left(\mathbf{W}_{\{i,l\}}\right)=\mathbf{0}$*, the second equality holds by choosing* $\mathbf{W}_{\{i,l\}}$ *such that* $\langle\mathscr{A}_{iL}^*\left(\mathbf{W}_{\{i,L\}}\right),\Delta\rangle=\|\mathscr{P}_{T_{kL}^{\perp}}\left(\mathbf{\Delta}_{\{k,L\}}\right)\|_*$*. The third equality is due to* $\mathscr{P}_{T_{il}^{\perp}}\left(\mathbf{R}_{\{i,l\}}\right)=\mathbf{0}$ *and* $\mathscr{P}_{\Omega^{\perp}}\left(\mathcal{Y}\right)=\mathscr{P}_{\Omega}\left(\Delta\right)=\mathcal{O}$*. The fourth inequality is because of (6) and hence*

$$
\begin{cases}
\langle\mathscr{P}_{T_{il}^{\perp}}\left(\mathbf{Y}_{\{i,l\}}\right),\mathscr{P}_{T_{il}^{\perp}}\left(\mathbf{\Delta}_{\{i,l\}}\right)\rangle\leq\dfrac{1}{2}\|\mathscr{P}_{T_{il}^{\perp}}\left(\mathbf{\Delta}_{\{k,l\}}\right)\|_* \\
\langle\mathbf{R}_{\{i,l\}}-\mathscr{P}_{T_{il}}\left(\mathbf{Y}_{\{i,l\}}\right),\mathscr{P}_{T_{il}}\left(\mathbf{\Delta}_{\{i,l\}}\right)\rangle\geq-\dfrac{1}{2}\displaystyle\prod_{k=1}^{d} n_k^{-1}\|\mathscr{P}_{T_{il}}\left(\mathbf{\Delta}_{\{i,l\}}\right)\|_{\mathrm{F}}
\end{cases}.
$$

The fifth inequality follows from the following deduction. Note that (5) indi-

cates

$$\begin{aligned}
&\langle \mathscr{P}_{T_{il}} \mathscr{P}_{\Omega_{il}} \mathscr{P}_{T_{il}} \left(\mathbf{\Delta}_{\{i,l\}} \right) - m \prod_{k=1}^{d} n_k^{-1} \mathscr{P}_{T_{il}} \left(\mathbf{\Delta}_{\{i,l\}} \right), \mathbf{\Delta}_{\{k,l\}} \rangle \\
\geq & - \| \mathscr{P}_{T_{il}} \mathscr{P}_{\Omega_{il}} \mathscr{P}_{T_{il}} \left(\mathbf{\Delta}_{\{i,l\}} \right) - m \prod_{k=1}^{d} n_k^{-1} \mathscr{P}_{T_{il}} \left(\mathbf{\Delta}_{\{i,l\}} \right) \|_{\mathrm{F}} \|\Delta\|_{\mathrm{F}} \\
\geq & - \frac{m}{2} \sqrt{\underline{n}_{il}} \prod_{k=1}^{d} n_k^{-1} \|\Delta\|_{\mathrm{F}},
\end{aligned}$$

where

$$\begin{aligned}
\langle \mathscr{P}_{T_{il}} \mathscr{P}_{\Omega_{il}} \mathscr{P}_{T_{il}} \left(\mathbf{\Delta}_{\{i,l\}} \right), \mathbf{\Delta}_{\{i,l\}} \rangle = & \| \mathscr{P}_{\Omega_{il}} \mathscr{P}_{T_{il}} \left(\mathbf{\Delta}_{\{i,l\}} \right) \|_{\mathrm{F}}^2 \\
= & \| \mathscr{P}_{\Omega_{il}} \mathscr{P}_{T_{il}^{\perp}} \left(\mathbf{\Delta}_{\{k,l\}} \right) \|_{\mathrm{F}}^2 \\
\leq & \| \mathscr{P}_{T_{il}^{\perp}} \left(\mathbf{\Delta}_{\{i,l\}} \right) \|_{\mathrm{F}}^2,
\end{aligned}$$

hence

$$\begin{aligned}
& \| \mathscr{P}_{T_{il}^{\perp}} \left(\mathbf{\Delta}_{\{i,l\}} \right) \|_{\mathrm{F}}^2 \\
\geq & \langle \mathscr{P}_{T_{il}} \mathscr{P}_{\Omega_{il}} \mathscr{P}_{T_{il}} \left(\mathbf{\Delta}_{\{i,l\}} \right), \mathbf{\Delta}_{\{i,l\}} \rangle \\
\geq & m \prod_{k=1}^{d} n_k^{-1} \left(\langle \mathscr{P}_{T_{il}} \left(\mathbf{\Delta}_{\{i,l\}} \right), \mathbf{\Delta}_{\{i,l\}} \rangle - \frac{1}{2} \sqrt{\underline{n}_{il}} \|\Delta\|_{\mathrm{F}} \right) \\
= & m \prod_{k=1}^{d} n_k^{-1} \left(\| \mathscr{P}_{T_{il}} \left(\mathbf{\Delta}_{\{i,l\}} \right) \|_{\mathrm{F}}^2 - \frac{1}{2} \sqrt{\underline{n}_{il}} \sqrt{\| \mathscr{P}_{T_{il}} \left(\mathbf{\Delta}_{\{i,l\}} \right) \|_{\mathrm{F}}^2 + \| \mathscr{P}_{T_{il}^{\perp}} \left(\mathbf{\Delta}_{\{i,l\}} \right) \|_{\mathrm{F}}^2} \right),
\end{aligned}$$

where the last equality follows from the Pythagorean identity. Therefore, by writing $a \triangleq \| \mathscr{P}_{T_{il}} \left(\mathbf{\Delta}_{\{i,l\}} \right) \|_{\mathrm{F}}^2$ *and* $b \triangleq \| \mathscr{P}_{T_{il}^{\perp}} \left(\mathbf{\Delta}_{\{i,l\}} \right) \|_{\mathrm{F}}^2$ *we have the quadratic*

inequality

$$a^2-\left(\frac{2}{m}\prod_{k=1}^{d}n_kb+\frac{\underline{n}_{kl}}{4}\right)a+\frac{1}{m^2}\prod_{k=1}^{d}n_k^2b^2-\frac{\underline{n}_{il}}{4}b\leq 0$$

whose discriminant follows $\triangle=\left(1+m^{-1}\prod_{k=1}^{d}n_k\right)b+\underline{n}_{il}^2/16>0$. *Then*

$$\begin{aligned}a\leq&\frac{1}{m}\prod_{k=1}^{d}n_kb+\frac{\underline{n}_{il}}{8}+\frac{1}{2}\sqrt{\triangle}\\ \leq&\frac{1}{m}\prod_{k=1}^{d}n_kb+\frac{\underline{n}_{il}}{4}+\left(1+\frac{1}{m}\prod_{k=1}^{d}n_k\right)\frac{b}{\underline{n}_{il}},\end{aligned}$$

which leads to

$$\begin{aligned}\|\mathscr{P}_{T_{il}^{\perp}}\left(\boldsymbol{\Delta}_{\{i,l\}}\right)\|_*\geq\|\mathscr{P}_{T_{il}^{\perp}}\left(\boldsymbol{\Delta}_{\{i,l\}}\right)\|_{\mathrm{F}}=\sqrt{b}\geq&\sqrt{\frac{m\prod_{k=1}^{d}n_k^{-1}\underline{n}_{il}\left(a-\frac{1}{4}\underline{n}_{il}\right)}{m\prod_{k=1}^{d}n_k^{-1}+\underline{n}_{il}+1}}\\ \geq&\sqrt{\prod_{k=1}^{d}n_k^{-2}a}\\ =&\prod_{k=1}^{d}n_k^{-1}\|\mathscr{P}_{T_{il}}\left(\boldsymbol{\Delta}_{\{i,l\}}\right)\|_{\mathrm{F}}.\end{aligned}$$

Hence, we prove for any $\Delta\neq\mathcal{O}$, $\mathscr{P}_{\Omega}(\Delta)=\mathcal{O}$ *there is* $\sum_{i=1}^{\lceil d/2\rceil}w_i\|\mathbf{X}_{\{i,l\}}+\Delta_{\{i,l\}}\|_*>\sum_{i=1}^{\lceil d/2\rceil}w_i\|\mathbf{X}_{\{i,l\}}\|_*$, *which indicates the uniqueness of the minimizer of (1). End of proof.* ■

5. Numerical Experiments

In this section, three groups of datasets are used for tensor completion experiments, i.e., synthetic data, real-world images and videos. To illustrate

the practical applicability of our model for tensor completion, the proposed model (1) is solved by alternating direction method of multipliers (ADMM) [23]. The corresponding algorithm is called tensor completion via tensor ring with balanced unfolding (TRBU). In each iteration of TRBU, the penalty parameter μ satisfies $\mu^k = \beta\mu^{k-1}$ with $\beta \in (0, 2)$ [24].

Eight algorithms are benchmarked on real-world data, including tensor ring nuclear norm minimization for tensor completion (TRNNM) [21], low rank tensor completion via alternating least square (TR-ALS) [18], simple low rank tensor completion via tensor train (SiLRTC-TT) [14], high accuracy low rank tensor completion algorithm (HaLRTC) [7], low rank tensor completion via tensor nuclear norm minimization (LRTC-TNN) [25], Bayesian CP Factorization (FBCP) for image recovery [26], smooth low rank tensor tree completion (STTC) [15] and the proposed one. These methods are based on different tensor decompositions, including CP, Tucker, t-SVD, HT, TT and TR decompositions. Table 1 shows the algorithmic complexity of eight algorithms, where d is the tensor dimension, n is the dimensional size, m is the number of samples and r ($[r, \ldots, r]$) is the tensor rank corresponding to each tensor decomposition.

Table 1: Comparison of complexity of eight algorithms in one iteration.

Algorithm	TRBU	TRNNM	TR-ALS	SiLRTC-TT
Complexity	$O\left(dn^{3d/2}\right)$	$O\left(dn^{3d/2}\right)$	$O\left(dmr^4\right)$	$O\left(dn^{3d/2}\right)$
Algorithm	LRTC-TNN	FBCP	HaLRTC	STTC
Complexity	$O\left(n^{d+1}\right)$	$O\left(dmr^2\right)$	$O\left(dn^{3d-3}\right)$	$O\left(dn^{d+1}\right)$

There are several metrics for evaluating the recovery quality of visual

data. The relative error (RE) is defined as $\text{RE} = \|\hat{\mathcal{X}} - \mathcal{X}\|_{\text{F}}/\|\mathcal{X}\|_{\text{F}}$, where $\mathcal{X}$ is the ground truth and $\hat{\mathcal{X}}$ is the estimate of $\mathcal{X}$. The peak signal-to-noise ratio (PSNR) is a ratio between the maximum possible power of a signal and the power of corrupting noise [27]. We use computational CPU time (in seconds) as a measure of algorithmic complexity.

The sampling rate (SR) is defined as the ratio of the number of samples to the total number of the elements of tensor $\mathcal{X}$, which is denoted as $\text{SR} = |\mathbb{O}|/|\mathcal{X}|$. For fair comparison, the parameters in each algorithm are tuned to give optimal performance. For the proposed TRBU algorithm, one of the stop criteria is that the relative change $\text{RC} = \|\mathcal{X}_k - \mathcal{X}_{k-1}\|_{\text{F}}/\|\mathcal{X}_{k-1}\|_{\text{F}}$ is less than a tolerance we set to 1×10^{-8}. We set the maximal number of iterations $K = 500$ in experiments on synthetic data and $K = 100$ in experiments on real-world data.

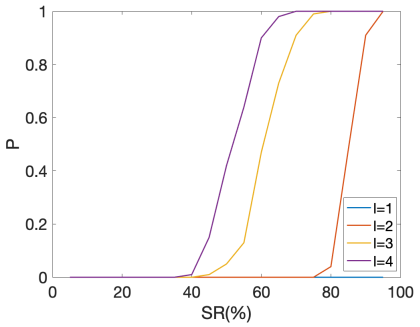
In the remainder of this section, we verify the theoretic analysis using synthetic data. The real-world data is also employed to test the proposed method, including images and videos. All the experiments are conducted in MATLAB 9.3.0 on a computer with a 2.8GHz CPU of Intel Core i7 and a 16GB RAM.

5.1. Exact Recovery from Random Problem

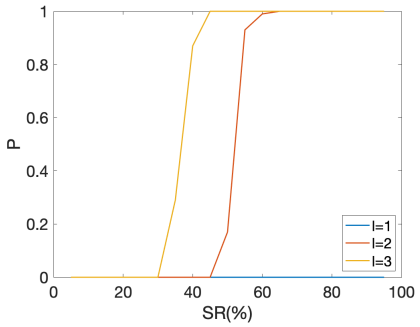
To testify Theorem 1, we generated two tensors in the first group of experiments: (a) a 8-order tensor $\mathcal{X} \in \mathbb{R}^{3\times\cdots\times 3}$ of TR rank $[2, \ldots, 2]$; (b) a 6-order tensor $\mathcal{X} \in \mathbb{R}^{6\times\cdots\times 6}$ of TR rank $[3, \ldots, 3]$. The entries of TR factors are independently sampled from the normal distribution $\mathcal{N}(0, 1/\sqrt{n})$. Their sampling rates range from 5% to 95% with linear interval 5%. For each tensor with different sampling rates, we run the TRBU algorithm 100 times to

recover its $d/2$ unfolding matrices, i.e., $\mathbf{X}_{\{1,l\}},\ l = 1, \ldots, d/2$. The parameter setting for proposed TRBU are $\beta = 1.028$ and $\mu_0 = 10^{-2.5}$.

The averaged results are shown in Fig. 1, which gives the recovery probabilities with respect to various sampling rates. In this experiment, a recovery is considered to be successful if RE $< 1 \times 10^{-6}$. It can be seen from Fig. 1 that a balanced unfolding matrix is easier to recover than an unbalanced one, which validates our claim that the more balance the matrix is, the easier it is to recover. Due to the superiority of TRBU when step length $l = \lceil d/2 \rceil$, we fix $l = \lceil d/2 \rceil$ in default in our later experiments.



(a) An 8-order tensor $\mathcal{X} \in \mathbb{R}^{3\times\cdots\times3}$ of TR rank $(2, \ldots, 2)$.



(b) A 6-order tensor $\mathcal{X} \in \mathbb{R}^{6\times\cdots\times6}$ of TR rank $(3, \ldots, 3)$.

Figure 1: Three experiments on randomly generated tensors.

In the second group of experiments, we generated two tensors, one with $d = 5$ and $n = 12$, the other with $d = 4$ and $n = 20$. The TR ranks are $[0.2n, \ldots, 0.2n]$ and $[0.3n, \ldots, 0.3n]$, respectively. The sampling rate is 0.1, 0.2, 0.3 and 0.4. We run the algorithm 10 times for each parameter setting. We set $\beta = 1.028$ and $\mu_0 = 10^{-2.5}$ for TRBU algorithm in this experiment.

Table 2 reports the recovery results of four scenarios. We examine the TR rank of the recovered tensor by computing rank $\left(\hat{\mathbf{L}}_{\{i,l\}}\right),\ i = 1, \ldots, d$,

$l = 1, \ldots, d-1$ and checking if they are equal to the square of the value of the pre-defined TR rank. In all cases, the relative error $\|\hat{\mathcal{L}} - \mathcal{L}_0\|_{\mathrm{F}} / \|\mathcal{L}_0\|_{\mathrm{F}}$ is less than 1×10^{-4}. Moreover, the TR ranks of the recovered tensors are consistent with the pre-defined ones, which illustrates the effectiveness of the proposed algorithm.

5.2. Phase Transition in TR rank with Varying Sampling Rates

In order to verify the recovery guarantee in Theorem 1, we generated a 4-order tensor $\mathcal{X} \in \mathbb{R}^{20 \times \cdots \times 20}$ by contracting independent TR factors whose entries are sampled from i.i.d. $\mathcal{N}\left(0, 1/\sqrt{20}\right)$ distributions. Theoretically, this tensor can be recovered successfully when $\mathrm{df}_{\mathrm{M}}/m < C$, where $\mathrm{df}_{\mathrm{M}} = r^2\left(2\sqrt{n^d} - r^2\right)$ is the degree of freedom (df) of a square unfolding and $C = O(1)$ is a constant. The df_{M} changing with sampling rate and TR rank are drawn in Fig. 2(a). The color of each cell represents the value of df_{M}.

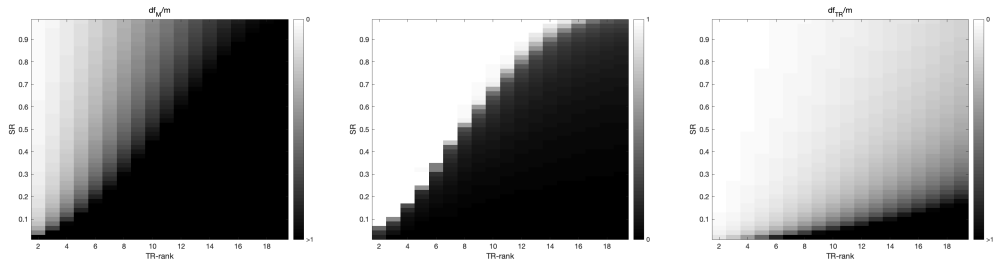
We vary TR rank from 2 to 19 to ensure df_{M} is positive. Then we carried out 10 experiments for each (SR, TR rank) pair, where the algorithmic parameters β and μ_0 are set to 1.028 and 10^{-2}, respectively. For each experiment, the recovery is considered to be successful if the relative error is less than 1×10^{-4}. The phase transition of the tensor completion is shown in Fig. 2(b), where the color bar reflects the empirical recovery rate which is scaled between 0 and 1. A white patch indicates a success of all experiments, while a black one represents a failure in all experiments.

The results show similar boundaries in Fig. 2(a) and Fig. 2(b), which is a validation for our main theory. As a comparison, the degree of freedom of the TR $\mathrm{df}_{\mathrm{TR}} = dnr^2 - dr^2 + 1$ [17] is plotted in Fig. 2(c), which suggests the sampling bound in Theorem 1 may be improved in some way since the

Table 2: Correct recovery results of a variety of randomly generated problems.

Size n	Order d	#samples m	$\operatorname{rank}(\mathcal{L}_0)$	$\operatorname{rank}\left(\hat{\mathcal{L}}\right)$	$\frac{\|\hat{\mathcal{L}}-\mathcal{L}_0\|_{\mathrm{F}}}{\|\mathcal{L}_0\|_{\mathrm{F}}}$	CPU time (s)
12	5	24884	2	2	5.27×10^{-6}	1.26×10^{1}
		49767	2	2	5.38×10^{-8}	1.16×10^{1}
20	4	16000	4	4	2.32×10^{-5}	1.41×10^{1}
		32000	4	4	6.31×10^{-8}	1.42×10^{1}
$\operatorname{rank}(\mathcal{L}_0) = \lfloor 0.2n \rfloor$ $(m = \lceil 0.1n^d \rceil$ *and* $\lceil 0.2n^d \rceil)$						
12	5	24884	3	3	3.17×10^{-6}	1.45×10^{1}
		49767	3	3	2.27×10^{-7}	1.54×10^{1}
20	4	16000	6	6	6.83×10^{-5}	2.11×10^{1}
		32000	6	6	6.88×10^{-7}	2.04×10^{1}
$\operatorname{rank}(\mathcal{L}_0) = \lfloor 0.3n \rfloor$ $(m = \lceil 0.1n^d \rceil$ *and* $\lceil 0.2n^d \rceil)$						
12	5	74650	2	2	7.70×10^{-8}	9.02×10^{0}
		99533	2	2	2.20×10^{-8}	6.30×10^{0}
20	4	48000	4	4	2.92×10^{-8}	1.01×10^{1}
		64000	4	4	2.21×10^{-8}	7.47×10^{0}
$\operatorname{rank}(\mathcal{L}_0) = \lfloor 0.2n \rfloor$ $(m = \lceil 0.3n^d \rceil$ *and* $\lceil 0.4n^d \rceil)$						
12	5	74650	3	3	5.17×10^{-8}	8.62×10^{0}
		99533	3	3	1.56×10^{-8}	5.64×10^{0}
20	4	48000	6	6	4.41×10^{-7}	1.95×10^{1}
		64000	6	6	1.64×10^{-8}	1.27×10^{1}
$\operatorname{rank}(\mathcal{L}_0) = \lfloor 0.3n \rfloor$ $(m = \lceil 0.3n^d \rceil$ *and* $\lceil 0.4n^d \rceil)$						

tensor cannot be recovered in the area where $\mathrm{df}_{\mathrm{M}}/m > C$ and $\mathrm{df}_{\mathrm{TR}}/m < C$.



(a) The ratio of degree of freedom of a square TR unfolding to the number of samples.

(b) The phase transition in TR rank with varying sampling rates.

(c) The ratio of degree of freedom of a TR to the number of samples.

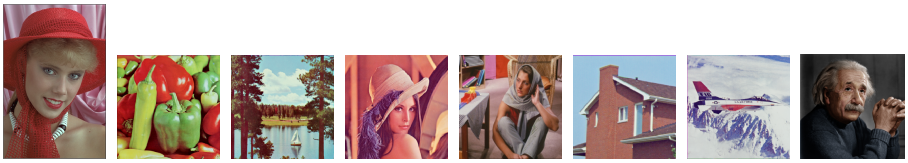
Figure 2: The completion result of a 4-order tensor $\mathcal{X} \in \mathbb{R}^{20\times\cdots\times 20}$ under various settings of TR ranks and sampling rates.

5.3. Color Images

The visual data tensorization (VDT) [28, 14] transforms an image into a real ket of a Hilbert space by an appropriate block structured addressing. For an image of size $M \times N \times 3$, VDT first reshapes it into a tensor of size $m_1 \times \cdots \times m_K \times n_1 \cdots \times n_K \times 3$, then permutes and reshapes the resulting tensor into another one with size $m_1 n_1 \times \cdots \times m_K n_K \times 3$.

Eight RGB images are used in the first group of experiments, including *kodim04* [2], *peppers*, *sailboat*, *lena*, *barbara*, *house*, *airplane* and *Einstein* [18]. The original images are shown in Fig. 3. To perform the experiments, we first apply VDT to these images. Specifically, we reshape *kodim04* by $[2 * \mathrm{ones}\,(1, 8)\,, 3, 2 * \mathrm{ones}\,(1, 9)\,, 3]$ and get a tensor of size $[4 * \mathrm{ones}\,(1, 8)\,, 6, 3]$. We reshape *Einstein* by $[2, 2, 2, 3, 5, 5, 5, 5, 3, 2, 2, 2, 3]$ and derive a tensor of

[2] http://r0k.us/graphics/kodak/kodim04.html



kodim04 *peppers* *sailboat* *lena* *barbara* *house* *air-plane* *Ein-stein*

Figure 3: The original copies of eight images.

size $[10, 10, 6, 6, 10, 10, 3]$. For other images, we reshape them into 17-order tensors of size $2 \times \cdots \times 2 \times 3$, further they are reshaped into 9-order tensors of size $4 \times \cdots \times 4 \times 3$. Note that the VDT is by manual operation and the result can change with the choice.

After the VDT operation, we compare the proposed algorithm with the state-of-the-art ones. The FBCP method needs a pre-defined maximal CP rank that is very time-consuming. Specifically, the maximum CP ranks are 50 for *kodim04*, 60 for *Einstein* and 100 for other images, otherwise the machine will be out of memory. The TR rank of all images is 14 for TR-ALS due to the computational source limit. The sampling rates for all images are from 10% to 90%. For each image with different sampling rate, we conducted 10 experiments, where the parameter setting are $\beta = 1.028$ and $\mu_0 = 1 \times 10^{-3.7}$.

As shown in Fig. 4, we compared the performance of eight algorithms both on completing the original low-order tensors and the high-order tensors from VDT processing. First, the performance of FBCP, HaLRTC, STTC and LRTC-TNN is very close in low order and high order cases by comparing Fig. 4(a) and Fig. 4(b). In addition, the TRBU, TRNNM, TR-ALS and SiLRTC-TT with VDT operation perform better than these without VDT, which shows that the TR decomposition and TT decomposition based methods are

more suitable for solving high-order data completion problems. Moreover, TR-ALS is the most time-consuming of all algorithms in all experiments. Since the TR rank is fixed, its performance does not improve as the sampling rate increases in high order case and we suspect the model is over-fitted [18], while an under-fitting problem occurs in low order case. When completing high-dimensional data, TRBU is superior to other algorithms in terms of PSNR, which shows the effectiveness of TRBU in the case of recovering high-order tensors.

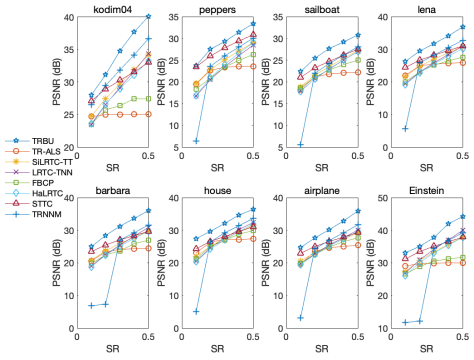
To simulate the non-uniform sampling situation, we use two RGB images in the second group of experiments, namely *house* and *llama*. The maximal CP rank for FBCP is 100. The TR rank used in TR-ALS is 14. We set $\beta = 1.028$ and $\mu_0 = 10^{-3}$ in this experiment.

The image recovery results for *house* and *llama* are shown in Fig. 5 and Fig. 6, respectively. The middle row shows the the recovery results of high-order tensor completions with VDT and the bottom row shows the recovery from directly completing the original images. Besides, it is apparent from Fig. 5 and Fig. 6 that TRBU is more capable of recovering high-order tensors.

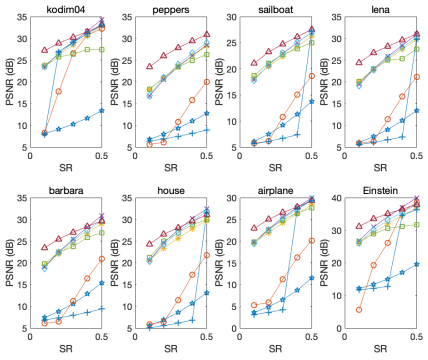
5.4. Real-world Videos

In this section we use two videos to test the algorithms and perform 5 experiments for each video. The first video called *explosion* is an explosion shot by a high speed camera [3]. We selected its 81st to 180th frames and downsampled each frame to size $80 \times 120 \times 3$. It is further converted into a

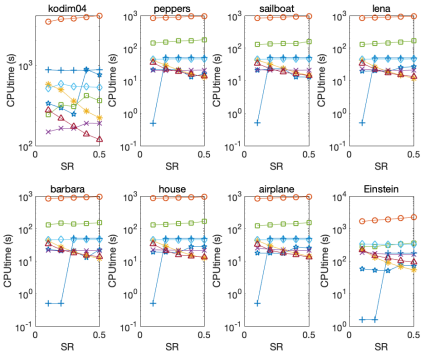
[3] http://www.newcger.com/shipinsucai/5786.html



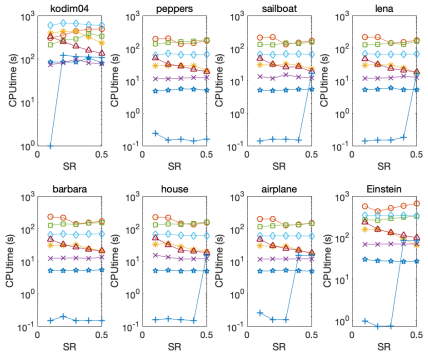
(a) Comparison of eight algorithms (with VDT operation) on PSNR (in dB).



(b) Comparison of eight algorithms (without VDT operation) on PSNR (in dB).



(c) Comparison of eight algorithms (with VDT operation) on CPU time (in seconds).



(d) Comparison of eight algorithms (without VDT operation) on CPU time (in seconds).

Figure 4: Recovery result of eight images based on eight algorithms.

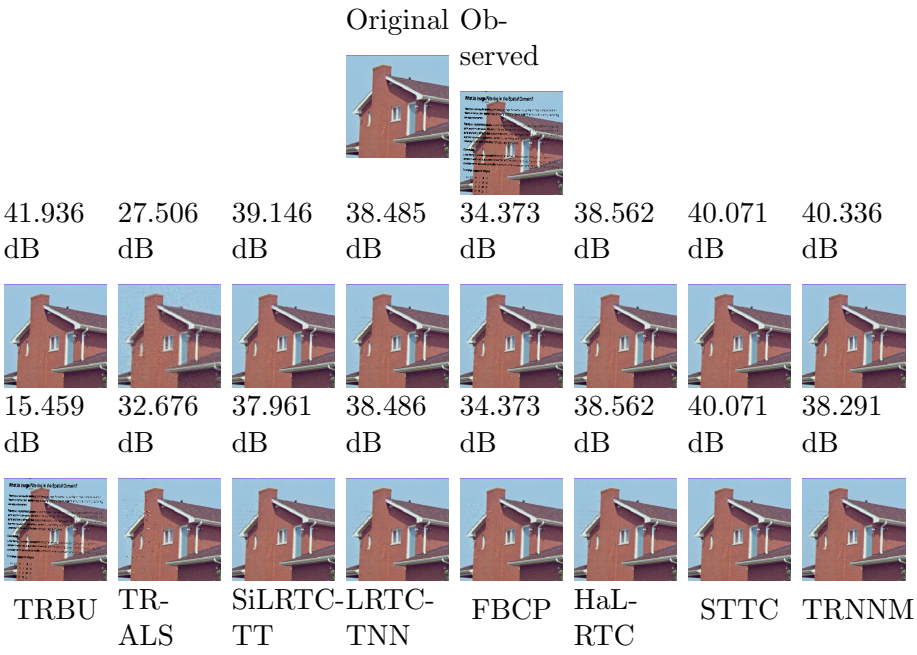


Figure 5: The recovery results of *house*, where the missing position is a text-like mask.

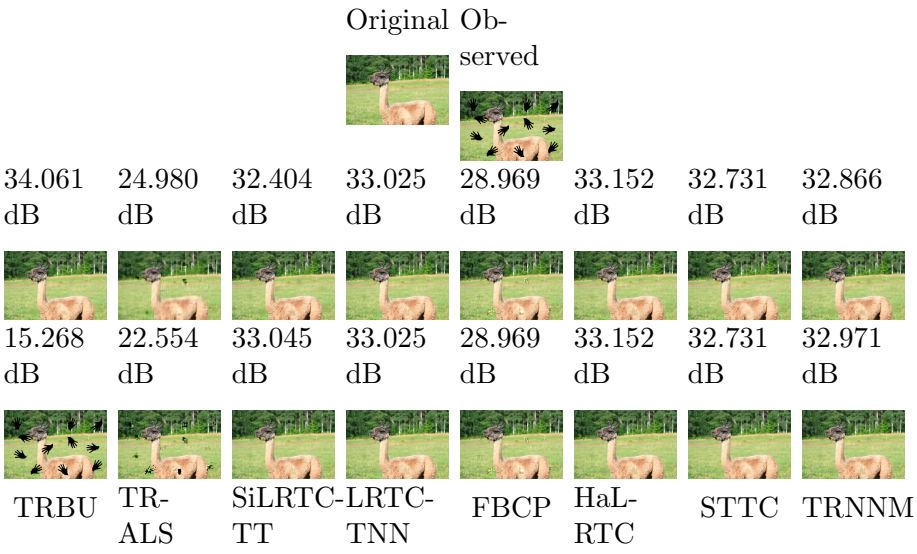


Figure 6: The recovery results of *llama*, where the missing positions are a few palm-shaped graffiti.

9-order tensor of size $8 \times 8 \times 4 \times 4 \times 10 \times 3 \times 4 \times 5 \times 5$ by VDT operation.

The second one is a color video that describes the activity of a bunch of chickens [4]. We downsampled each frame to size $72 \times 128 \times 3$ and finally get a tensor of size $8 \times 8 \times 4 \times 6 \times 6 \times 3 \times 4 \times 5 \times 5$ by VDT manipulation. The TR rank for TR-ALS is 12 due to machine memory limit. The maximal CP rank for FBCP is limited by 40. The sampling rate of two videos is 10%. We set $\beta = 1.05$ and $\mu_0 = 1 \times 10^{-3.7}$ in this experiment.

We conducted the experiments for two whole videos. For each video, we show the recovery result of one frame in Fig. 7 and Fig. 8. The middle row shows the recovery results for high-order tensor completion using VDT, and the bottom row shows the recovery results, in which case the original images are directly completed. The limited CP rank may deteriorate the performances of FBCP. This also implies huge storage requirement of FBCP. The TR-ALS is unable to effectively handle large scale data since it costs too much time. The TRBU has much better recovery quality among all methods and is efficient at large scale data completion.

6. Conclusion

We study the tensor ring decomposition and propose a weighted sum of nuclear norm minimization model for tensor ring completion. Meanwhile, a recovery guarantee for TR completion under random sampling scheme is provided and proved. To verify the effectiveness of the proposed model, a method based on ADMM, namely TRBU, is proposed to tackle this problem. The results of experiments on synthetic data not only verify the pro-

[4] https://pixabay.com/videos/id-10685/

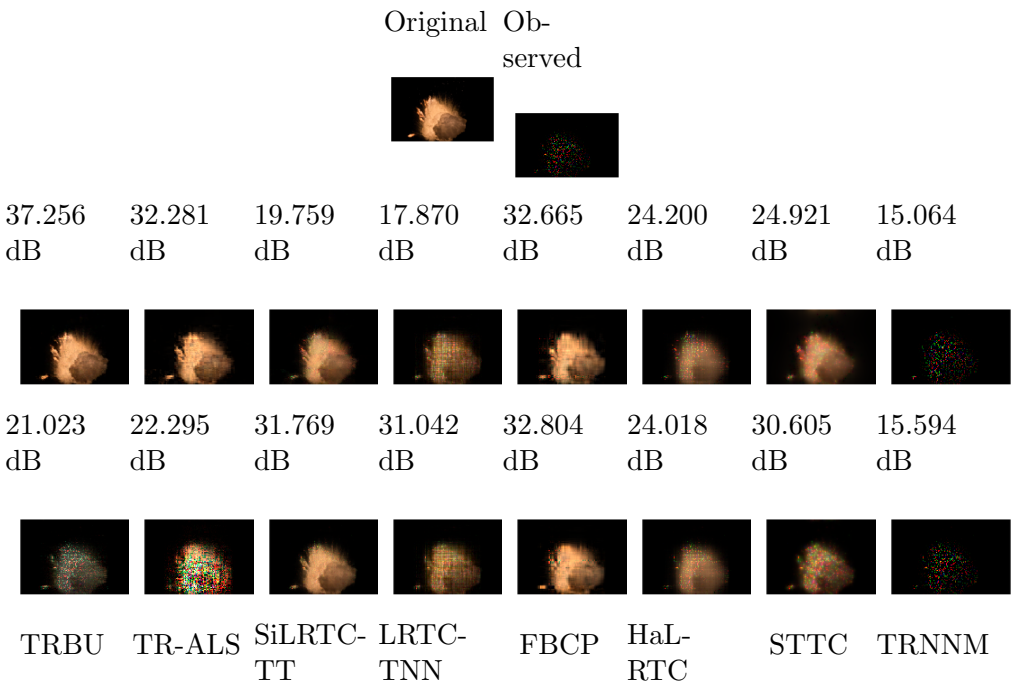


Figure 7: The recovery results of the last frame of *explosion*, where the evaluation is based on the whole video.

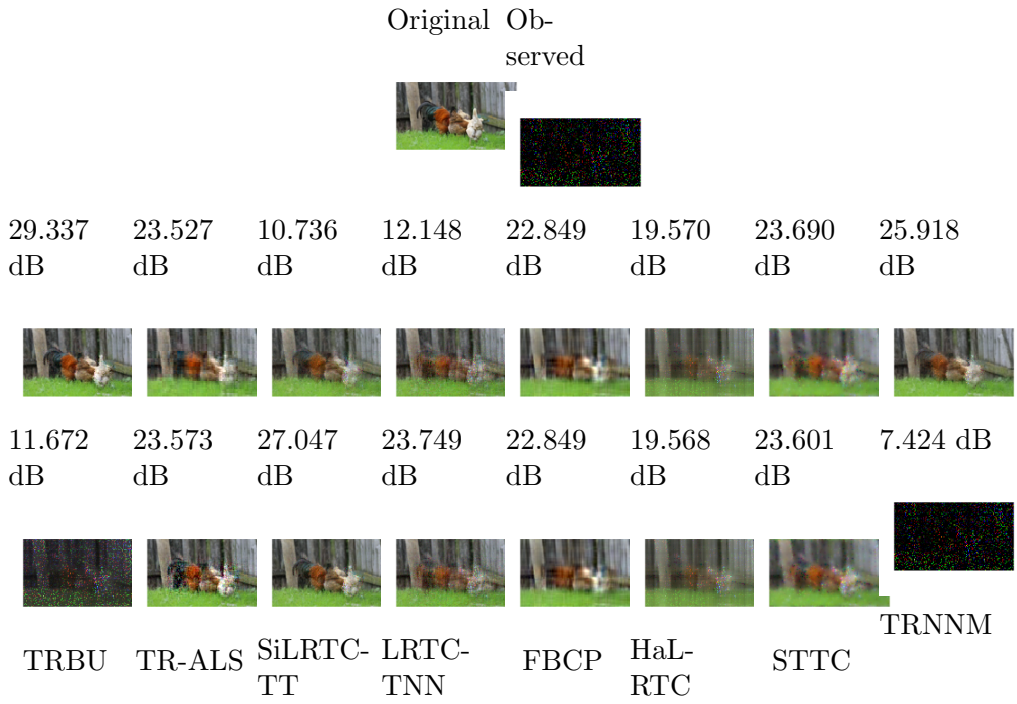


Figure 8: The recovery results of the first frame of *cock*, where the evaluation is based on the whole video.

posed sampling condition for TR completion but also show that the sampling bound is conservative and can be improved, which will become our future work. Experiments on real-world data further demonstrate the efficiency of TRBU over other state-of-art algorithms, especially for higher-order tensor completion.

Appendix A. Proof of Lemma 1

Proof. *We first recall a concentration-of-measure inequality that is important for our analysis.*

Lemma 4 (McDiarmid inequality [29])**.** *Let* $\{X_1, \ldots, X_n\}$ *be independent random variables such that there are* $a_i \leq X_i \leq b_i$, $c_i := b_i - a_i$ *and* $c_i \leq C$, $\forall i = 1, \ldots, n$. *Let* S *be an arbitrary (implicit) function of the variables, e.g., the sum function, then for any* $t > 0$ *there is*

$$\mathrm{P}\left(|S - \mathrm{E}\left(S\right)| > t\right) < 2e^{-\frac{2t^2}{nC^2}}, \tag{A.1}$$

as long as this function changes in a bounded way, i.e., if X_i *is changed, the value of this function changes by at most* C.

We consider the i-th TR factor $\mathcal{G}^{(i)}$. *According to the identity* $\sum_{j_i=1}^{n_i} H_{j_i}^2 = 1$, *there is* $\mathrm{E}\left(H_{j_i}^2\right) = 1/n_i$, *supposing that* $H_{j_i} = \mathcal{G}_{tj_is}^{(i)}$. *Let* $X_{ts} = \mathcal{G}_{tj_is}^{(i)} \mathcal{G}_{tj_i's}^{(i)}$ *and* $S = \sum_t \sum_s X_{ts}$, *obviously* $\mathrm{E}\left(S\right) = 0$ *if* $j_i \neq j_i'$, *and we have* $\mathrm{E}\left(S\right) = \sum_{t=1}^{r_i} \sum_{s=1}^{r_{i+1}} \mathrm{E}\left(H_{j_i}^2\right) = r_i r_{i+1}/n_i$ *if* $j_i = j_i'$.

The proof is as follows. From the above deductions it is clear that $\mathrm{E}\left(S\right) = \frac{r_i r_{i+1}}{n_i} 1_{j_i = j_i'}$. *According to the union bound* $\max\left(\mathcal{G}^{(i)}\right) \leq \sqrt{\frac{\mu_{B_i}}{n_i}}$, *the bound of* X_{ts} *is* $C = 2\frac{\mu_{B_i}}{n_i}$. *Incorporating Lemma 4 we have* $\Pr\left(|\langle \mathcal{G}_{:j_i:}^{(i)}, \mathcal{G}_{:j_i':}^{(i)} \rangle - \frac{r_i r_{i+1}}{n_i} 1_{j_i = j_i'}| > \frac{\lambda \mu_{B_i} \sqrt{r_i r_{i+1}}}{n_i}\right) <$

$2e^{-\frac{\lambda^2}{2}}$, *and let* λ *be a proportion of* $\sqrt{\ln(n_i)}$ *we prove (2) with probability at least* $1-n_i^{-3}$ *(say). Additionally, there is* $\mu_i = O\left(\mu_{B_i}\sqrt{\ln(n_i)}\right)$.

Note that the above result is only for one core of TR, the total probability is $\prod_{i=1}^{d}\left(1-n_i^{-3}\right)$. ■

Appendix B. Proof of Lemma 2

Proof. *We use the first formulation of TR decomposition, i.e.,* $x_{j_1\cdots j_d} = \mathrm{tr}\left(\mathbf{\Sigma}^{(1)}\mathbf{G}_{j_1}^{(1)}\cdots\ \mathbf{\Sigma}^{(d)}\mathbf{G}_{j_d}^{(d)}\right)$. *Note that every mode-2 slice of* $\mathcal{G}^{(i)}$ *has the same status when interacting with* $\mathbf{\Sigma}_i$ *and* $\mathbf{\Sigma}_{i+1}$*, then a substitution for the representation of TR factors is* $\widetilde{\mathcal{G}}^{(i)} = \mathcal{W}^{(i)}\circledast\mathcal{G}^{(i)}$*, where* $\mathcal{W}_{:j_i:}^{(i)} = \mathrm{diag}\left(\sqrt{\mathbf{\Sigma}_i}\right)\mathrm{diag}\left(\sqrt{\mathbf{\Sigma}_{i+1}}\right)^{\mathrm{T}}$ *holds for all mode-2 slices of* $\mathcal{W}^{(i)}$*. We use matrix* $\mathbf{W}^{(i)}$ *to denote any mode-2 slice of* $\mathcal{W}^{(i)}$ *for convenience.*

We consider a 4-order tensor and calculate the SVD for its TR unfolding. For simplicity, we denote by $\mathbf{U}$ *the* s_1*-th mode-1 slice of* $\widetilde{\mathcal{G}}^{(1)}$ *and* $\mathbf{V}$ *the* t_3*-th mode-3 slice of* $\widetilde{\mathcal{G}}^{(2)}$*. Consequently, the* ℓ_2*-norm of the mode-2 fiber of* $\widetilde{\mathcal{G}}^{(1)}\overline{\otimes}\widetilde{\mathcal{G}}^{(2)}$ *is*

$$\begin{aligned}\sqrt{\sum_i\sum_j\left(\mathbf{U}\mathbf{V}^{\mathrm{T}}\right)_{ij}^2} &= \sqrt{\sum_k w_{s_1k}^{(1)}w_{kt_3}^{(2)}\sum_{k'}w_{s_1k'}^{(1)}w_{k't_3}^{(2)}\sum_i u_{ik}u_{ik'}\sum_j v_{jk}v_{jk'}}\\ &= \left(\mathbf{W}^{(1)}\mathbf{W}^{(2)}\right)_{s_1t_3}\end{aligned}$$

by using the orthonormal condition of $\mathbf{U}$ *and* $\mathbf{V}$*. Thus the* ℓ_2*-norms of mode-2 fibers of* $\widetilde{\mathcal{G}}^{(1)}\overline{\otimes}\widetilde{\mathcal{G}}^{(2)}$ *are* $\mathbf{W}^{(1)}\mathbf{W}^{(2)} = \mathrm{tr}\left(\mathbf{\Sigma}_2\right)\mathrm{diag}\left(\sqrt{\mathbf{\Sigma}_1}\right)\mathrm{diag}\left(\sqrt{\mathbf{\Sigma}_3}\right)^{\mathrm{T}}$ *and the representation of the TR unfolding is*

$$\mathbf{X}_{\{1,2\}} = \left[\left(\mathcal{W}^{(1)}\overline{*}\mathcal{W}^{(2)}\right)\circledast\mathcal{U}^{\{1,2\}}\right]_{(2)'}\left[\left(\mathcal{W}^{(3)}\overline{*}\mathcal{W}^{(4)}\right)\circledast\mathcal{V}^{\{3,2\}}\right]_{(2)}^{\mathrm{T}},$$

where $\overline{*}$ *is the slice-wise matrix product acting on corresponding mode-2 slices, operators* $(\cdot)_{(2)'}$ *and* $(\cdot)_{(2)}$ *unfold a TR factor into a matrix with permuted order* $[2,3,1]^{\mathrm{T}}$ *and* $[2,1,3]^{\mathrm{T}}$*, respectively. We derive* $\mathbf{X}_{\{1,2\}} = \mathcal{U}_{(2)'}^{\{1,2\}} \mathbf{\Sigma}_{13} \mathcal{V}_{(2)}^{\{3,2\}^{\mathrm{T}}}$*, where* $\mathcal{U}^{\{1,2\}} = \mathcal{G}^{(1)} \overline{\otimes} \mathcal{G}^{(2)}$*,* $\mathcal{V}^{\{3,2\}} = \mathcal{G}^{(3)} \overline{\otimes} \mathcal{G}^{(4)}$ *and*

$$
\begin{aligned}
\mathbf{\Sigma}_{13} &= \operatorname{diag}\left(\overrightarrow{\left(\mathbf{W}^{(1)}\mathbf{W}^{(2)}\right)}\right) \circledast \operatorname{diag}\left(\downarrow\left(\mathbf{W}^{(3)}\mathbf{W}^{(4)}\right)\right) \\
&= \operatorname{tr}\left(\mathbf{\Sigma}_2\right) \operatorname{diag}\left(\overrightarrow{\left(\operatorname{diag}\left(\sqrt{\mathbf{\Sigma}_1}\right) \operatorname{diag}\left(\sqrt{\mathbf{\Sigma}_3}\right)^{\mathrm{T}}\right)}\right) \circledast \\
&\quad \operatorname{tr}\left(\mathbf{\Sigma}_4\right) \operatorname{diag}\left(\downarrow\left(\operatorname{diag}\left(\sqrt{\mathbf{\Sigma}_3}\right) \operatorname{diag}\left(\sqrt{\mathbf{\Sigma}_1}\right)^{\mathrm{T}}\right)\right) \\
&= \operatorname{tr}\left(\mathbf{\Sigma}_2\right) \operatorname{tr}\left(\mathbf{\Sigma}_4\right) \operatorname{diag}\left(\downarrow\left(\sqrt{\boldsymbol{\sigma}_3}\sqrt{\boldsymbol{\sigma}_1}^{\mathrm{T}}\right)\right) \circledast \\
&\quad \operatorname{diag}\left(\downarrow\left(\sqrt{\boldsymbol{\sigma}_3}\sqrt{\boldsymbol{\sigma}_1}^{\mathrm{T}}\right)\right) \\
&= \operatorname{tr}\left(\mathbf{\Sigma}_2\right) \operatorname{tr}\left(\mathbf{\Sigma}_4\right) \operatorname{diag}\left(\left(\sqrt{\boldsymbol{\sigma}_1} \otimes \sqrt{\boldsymbol{\sigma}_3}\right) \circledast \left(\sqrt{\boldsymbol{\sigma}_1} \otimes \sqrt{\boldsymbol{\sigma}_3}\right)\right) \\
&= \operatorname{tr}\left(\mathbf{\Sigma}_2\right) \operatorname{tr}\left(\mathbf{\Sigma}_4\right) \operatorname{diag}\left(\boldsymbol{\sigma}_1 \otimes \boldsymbol{\sigma}_3\right) \\
&= \operatorname{tr}\left(\mathbf{\Sigma}_2\right) \operatorname{tr}\left(\mathbf{\Sigma}_4\right) \mathbf{\Sigma}_1 \otimes \mathbf{\Sigma}_3.
\end{aligned}
$$

Here the operator $\downarrow(\cdot) := \operatorname{vec}(\cdot)$ *rearranges a matrix into a vector column by column and* $\overrightarrow{(\cdot)} := \operatorname{vec}\left(\cdot^{\mathrm{T}}\right)$ *rearranges a matrix into a vector row by row. To determine the rank of* $\mathbf{X}_{\{1,2\}}$*, we have* $\operatorname{rank}\left(\mathbf{\Sigma}_{13}\right) = \operatorname{rank}\left(\mathbf{\Sigma}_1\right) \operatorname{rank}\left(\mathbf{\Sigma}_3\right) = r_1 r_3$.

The next step is to verify the orthogonality of $\mathcal{U}^{\{1,2\}}$ *and* $\mathcal{V}^{\{3,2\}}$*. Since*

$$
\sum_k w_{r_1 k}^{(1)} w_{k r_3}^{(2)} \sum_t w_{r_1 t}^{(1)} w_{t r_3}^{(2)} \sum_i u'_{ik} u''_{it} \sum_j v'_{jk} v''_{jt} \equiv 0,
$$

where $\mathbf{U}' \neq \mathbf{U}''$ *or* $\mathbf{V}' \neq \mathbf{V}''$*, which means two pairs of slices are not allowed*

to be the same at the same time. With this expression it is clear that both $\mathcal{U}^{\{1,2\}} = \mathcal{G}^{(1)} \overline{\otimes} \mathcal{G}^{(2)}$ *and* $\mathcal{V}^{\{3,2\}} = \mathcal{G}^{(3)} \overline{\otimes} \mathcal{G}^{(4)}$ *are orthogonal.*

Generally there are $\mathbf{X}_{\{k,l\}} = \mathcal{U}_{(2)'}^{\{k,l\}} \mathbf{\Sigma}_{k,k+l} \mathcal{V}_{(2)}^{\{k+l,d-l\}^{\mathrm{T}}}$, *where* $\mathcal{U}^{\{k,l\}} = \overline{\otimes}_{i=k}^{k+l-1} \mathcal{G}^{(i)}$, $\mathcal{V}^{\{k+l,d-l\}} = \overline{\otimes}_{i=k+l}^{k-1} \mathcal{G}^{(i)}$ *and* $\mathbf{\Sigma}_{k,k+l} = \prod_{i \neq k,\, k+l} \operatorname{tr}(\mathbf{\Sigma}_i)\, \mathbf{\Sigma}_k \otimes \mathbf{\Sigma}_{k+l}$. *The rank is given by* $\operatorname{rank}\left(\mathbf{X}_{\{k,l\}}\right) = r_k r_{k+l}$.

To calculate the ℓ_2*-norm of the mode-2 fiber of* $\overline{\otimes}_{k=n}^{n+l-1} \mathcal{G}^{(k)}$, *we consider a simple case in which two factors are contracted. The* (r_1, r_3)*-th mode-2 fiber of* $\mathcal{G}^{(1)} \overline{\otimes} \mathcal{G}^{(2)}$ *can be written as* $\left(\mathcal{G}^{(1)} \overline{\otimes} \mathcal{G}^{(2)}\right)_{r_1 : r_3} = \downarrow \left(\mathcal{G}_{r_1 ::}^{(1)} \mathcal{G}_{::r_3}^{(2)}\right)$, *and hence the* ℓ_2*-norm of the fiber is equal to the* F*-norm of the matrix which is* $\|\mathcal{G}_{r_1 ::}^{(1)} \mathcal{G}_{::r_3}^{(2)}\|_{\mathrm{F}} = \|\mathbf{E}_{r_2}\|_{\mathrm{F}} = r_2$. *This equation is because mode-2 fibers of* $\mathcal{G}^{(1)}$ *and* $\mathcal{G}^{(2)}$ *are orthonormal. Let* $\mathcal{G}^{(1)} \overline{\otimes} \mathcal{G}^{(2)}$ *be a contracted factor and recursively repeat the above procedure, we prove that the* ℓ_2*-norm of the mode-2 fiber of* $\overline{\otimes}_{i=k}^{k+l-1} \mathcal{G}^{(i)}$ *is* $\prod_{i=k+1}^{k+l-1} r_i$. *Therefore, the left and right singular matrices of* $\mathbf{X}_{\{k,l\}}$ *are* $\mathcal{U}^{\{k,l\}} = \prod_{i=k+1}^{k+l-1} \frac{1}{r_i} \overline{\otimes}_{i=k}^{k+l-1} \mathcal{G}^{(i)}$ *and* $\mathcal{V}^{\{k+l,d-l\}} = \prod_{i=k+l+1}^{k-1} \frac{1}{r_i} \overline{\otimes}_{i=k+l}^{k-1} \mathcal{G}^{(i)}$.

Subsequently, we calculate the variable expectation. Similar to the proof of Definition 1, let $H_{s\bar{i}t} = \left(\overline{\otimes}_{i=k}^{k+l-1} \mathcal{G}^{(i)}\right)_{s\bar{i}t} = \left(\prod_{i=k}^{k+l-1} \mathcal{G}_{:i_k:}^{(i)}\right)_{st}$, *there is* $\mathrm{E}\left(H_{s\bar{i}t}^2\right) = \prod_{i=k+1}^{k+l-1} r_i^2 / \prod_{i=k}^{k+l-1} n_i$, *where* $\bar{i} \in \left\{1, \ldots, 1 + \sum_{i=k}^{k+l-1} (n_i - 1) \prod_{j=i}^{i-1} n_j\right\}$. *We define* $S = \langle \mathcal{U}_{:\bar{i}:}, \mathcal{U}_{:\bar{j}:} \rangle = \langle \left(\overline{\otimes}_{i=k}^{k+l-1} \mathcal{G}^{(i)}\right)_{:\bar{i}:}, \left(\overline{\otimes}_{i=k}^{k+l-1} \mathcal{G}^{(i)}\right)_{:\bar{j}:} \rangle = \sum_s \sum_t H_{s\bar{i}t} H_{s\bar{j}t}$, *then* $\mathrm{E}(S) = \left(r_k r_{k+l} \prod_{i=k}^{k+l-1} r_i^2 \prod_{i=k}^{k+l-1} n_i^{-1}\right) 1_{i=j}$, *where the definition of* j *is the same with that of* i *above. Performing the normalization we have a modification* $\mathrm{E}(S) = \left(r_k r_{k+l} \prod_{i=k}^{k+l-1} n_i^{-1}\right) 1_{i=j}$.

Assuming that only two factors are allowed to be contracted at a time and we start the contraction from the k*-th core. Notice the normalization, and the variable bound can be calculated by the following recursive formula* $C_{\{k,l\}} =$

$C_{\{k,l-1\}}\frac{\mu_{B_{k+l-1}}}{n_{k+l-1}}$, *where* $C_{\{k,1\}}=2\frac{\mu_{B_k}}{n_k}$. *This implies* $C_{\{k,l\}}=2\prod_{i=k}^{k+l-1}\frac{\mu_{B_i}}{n_i}$. *It is trivial to verify that* $C_{\{k,l\}}<C_{\{k,1\}}$ *for enough large* $\{n_i\}$.

According to Lemma 4, we have $\Pr\left(|\langle\mathcal{U}_{:\bar{i}:}^{\{k,l\}},\mathcal{U}_{:\bar{j}:}^{\{k,l\}}\rangle-\frac{r_kr_{k+l}}{\prod_{i=k}^{k+l-1}n_i}1_{\bar{i}=\bar{j}}|>t\right)<2e^{-\frac{2t^2}{r_kr_{k+l}C_{\{k,l\}}^2}}$. *Let* $t=\lambda\sqrt{r_kr_{k+l}}\prod_{i=k}^{k+l-1}\frac{\mu_{B_i}}{n_i}$, *the right term becomes* $2e^{-\frac{\lambda^2}{2}}$. *Choosing* $\lambda=O\left(\sqrt{\sum_{i=k}^{k+l-1}\ln n_i}\right)$, *inequality* $|\langle\mathcal{U}_{:\bar{i}:}^{\{k,l\}},\mathcal{U}_{:\bar{j}:}^{\{k,l\}}\rangle-\frac{r_kr_{k+l}}{\prod_{i=k}^{k+l-1}n_i}1_{\bar{i}=\bar{j}}|\leq\lambda\sqrt{r_kr_{k+l}}\prod_{i=k}^{k+l-1}\frac{\mu_{B_i}}{n_i}$ *holds with probability at least* $1-\prod_{i=k}^{k+l-1}n_i^{-3}$.

The proof of inequality about $\mathcal{V}^{\{k+l,d-l\}}$ *is similar to that of* $\mathcal{U}^{\{k,l\}}$ *and hence is skipped.*

Let $X_{st}=\left(\overline{\otimes}_{i=k}^{k+l-1}\mathcal{G}^{(i)}\right)_{s\bar{i}t}\left(\overline{\otimes}_{i=k+l}^{k-1}\mathcal{G}^{(i)}\right)_{s\bar{j}t}$, *it is evident that* $\mathrm{E}(X_{st})\equiv 0$, *and the variable bound satisfies* $C=C_{\{k,l\}}C_{\{k+l,d-l\}}=2\prod_{i=1}^{d}\frac{\mu_{B_i}}{n_i}$. *Plugging* $t=\sqrt{r_kr_{k+l}}\prod_{i=1}^{d}\mu_{B_i}n_i^{-1/2}$ *into* $\Pr\left(|\langle\mathcal{U}_{:\bar{i}:}^{\{k,l\}},\mathcal{V}_{:\bar{j}:}^{\{k+l,d-l\}}\rangle|>t\right)<2e^{-\frac{2t^2}{r_kr_{k+l}C^2}}$, *we prove* $|\langle\mathcal{U}_{:\bar{i}:}^{\{k,l\}},\mathcal{V}_{:\bar{j}:}^{\{k+l,d-l\}}\rangle|\leq\frac{\sqrt{r_kr_{k+l}}\prod_{i=1}^{d}\mu_{B_i}}{\prod_{i=1}^{d}\sqrt{n_i}}$ *holds with probability at least* $1-e^{-\frac{1}{2}\prod_{i=1}^{d}n_i}$.

With the above deduction, the following inequalities

$$\begin{cases}|\langle\mathcal{U}_{:\bar{i}:}^{\{k,l\}},\mathcal{U}_{:\bar{j}:}^{\{k,l\}}\rangle-\dfrac{r_kr_{k+l}}{\prod_{i=k}^{k+l-1}n_i}1_{\bar{i}=\bar{j}}|\leq\dfrac{\mu'_{1kl}\sqrt{r_kr_{k+l}}}{\prod_{i=k}^{k+l-1}n_i}\\ |\langle\mathcal{V}_{:\bar{i}:}^{\{k+l,d-l\}},\mathcal{V}_{:\bar{j}:}^{\{k+l,d-l\}}\rangle-\dfrac{r_kr_{k+l}}{\prod_{i=k+l}^{k-1}n_i}1_{\bar{i}=\bar{j}}|\leq\dfrac{\mu'_{2kl}\sqrt{r_kr_{k+l}}}{\prod_{i=k+l}^{k-1}n_i}\end{cases}$$

hold with probabilities at least $1-\prod_{i=k}^{k+l-1}n_i^{-3}$ *and* $1-\prod_{i=k+l}^{k-1}n_i^{-3}$, *respectively. Inequality* $|\langle\mathcal{U}_{:\bar{i}:}^{\{k,l\}},\mathcal{V}_{:\bar{j}:}^{\{k+l,d-l\}}\rangle|\leq\frac{\mu''\sqrt{r_kr_{k+l}}}{\sqrt{\prod_{i=1}^{d}n_i}}$ *holds with probability at least* $1-$

$e^{-\frac{1}{2}\prod_{i=1}^{d} n_i}$, *where*

$$\begin{cases} \mu'_{1kl} = O\left(\prod\limits_{i=k}^{k+l-1} \mu_{B_i} \sqrt{\sum\limits_{i=k}^{k+l-1} \ln n_i}\right),\ \mu'_{2kl} = O\left(\prod\limits_{i=k+l}^{k-1} \mu_{B_i} \sqrt{\sum\limits_{i=k+l}^{k-1} \ln n_i}\right) \\ \mu'' = \prod\limits_{i=1}^{d} \mu_{B_i} \end{cases}$$

The proof is end. ■

Appendix C. Proof of Lemma 3

Proof. *Since Lemma 2 indicates a TR unfolding has a unique SVD, we define the linear spaces* $T_{il} = \{\mathbf{T} | \mathbf{T} = \prod_{k=i+1}^{i+l-1} \frac{1}{r_k} \mathcal{U}_{(2)'}^{\{i,l\}} \mathbf{Y}^{\mathrm{T}} + \prod_{k=i+l+1}^{i-1} \frac{1}{r_k} \mathbf{X} \mathcal{V}_{(2)}^{\{i,l\}^{\mathrm{T}}},\ \forall\, \mathbf{X}, \mathbf{Y} \in \mathbb{R}^{\prod_{k=i}^{i+l-1} n_k \times \prod_{k=i+l}^{i-1} n_k}\}$ *and* $T_{il}^{\perp}$ *as the orthogonal complement of* T_{il}*. The formulations of orthogonal projections* $\mathscr{P}_{T_{il}}$ *and* $\mathscr{P}_{T_{il}^{\perp}} = \mathscr{I} - \mathscr{P}_{T_{il}}$ *are* $\mathscr{P}_{T_{il}}(\mathbf{X}) = \mathscr{P}_{U_{il}}\mathbf{X} + \mathbf{X}\mathscr{P}_{V_{il}} - \mathscr{P}_{U_{il}}\mathbf{X}\mathscr{P}_{V_{il}}$ *and* $\mathscr{P}_{T_{il}^{\perp}}(\mathbf{X}) = (\mathscr{I} - \mathscr{P}_{U_{il}})\,\mathbf{X}\,(\mathscr{I} - \mathscr{P}_{V_{il}})$*, respectively.*

To prove (5), we verify it with the Rudelson selection estimate [30] under the assumption of strong TR incoherence condition. Since $\|\mathscr{P}_{T_{il}}\mathscr{P}_{\Omega_{il}}\mathscr{P}_{T_{il}} - p\mathscr{P}_{T_{il}}\|_2 \leq ap$ *with probability at least* $1 - 3\overline{n}_{il}^{-\beta}$ *for any* $\beta > 1$ *and* $a = C_R\sqrt{\mu_0 \overline{n}_{il} r_i r_{i+l} \beta \ln(\overline{n}_{il})/m} < 1$*, note that* $\mu_0 \leq 1 + \max\{\mu_{1il}, \mu_{2il}\}/\sqrt{r_i r_{i+l}} \leq 1 + \mu_{il}/\sqrt{r_i r_{i+l}}$*. Applying this theorem with* $a = 1/2$ *and* $\beta = 4$ *gives the validation of (5), where* m *is required to be larger than* $\max_i C\mu\overline{n}_{il} r_i r_{i+l} \ln(\overline{n}_{il})$*. The proof to (5) is complete.*

To prove the first condition in (6), we construct the dual certificate via the Golf scheme introduced in [31]. Considering a union of Ω *where* $\Omega = \cup_{j=1}^{j_0} \Omega^j$ *and* $j_0 = \lfloor \frac{5}{2}\log_2(\overline{n}_{kl}) + 1 \rfloor$*, and each* Ω^j *obeys the Bernoulli model* $\Omega^j \sim$

$\mathrm{Ber}\left(q_j\right)$ *where* $q_j = 1-(1-p)^{1/j_0}$, $p = m\prod_{i=1}^{d} n_i^{-1}$. *Inductively defining*

$$\begin{cases} \mathbf{Z}_{\{i,l\}}^{0} = \mathcal{U}_{(2)'}^{\{i,l\}} \mathcal{V}_{(2)}^{\{i+l,d-l\}^{\mathrm{T}}} = \mathscr{R}\left(\{\mathcal{G}\}\right)_{\{i,l\}} \\ \mathbf{Y}_{\{i,l\}}^{j} = \sum_{k=1}^{j} q_k^{-1} \mathscr{P}_{\Omega_{il}^{k}} \mathscr{P}_{T_{il}} \left(\mathbf{Z}_{\{i,l\}}^{k-1}\right) \qquad , \ i = 1, \ldots, \lceil d/2 \rceil, \\ \mathbf{Z}_{\{i,l\}}^{j} = \mathbf{Z}_{\{i,l\}}^{0} - \mathscr{P}_{T_{il}} \left(\mathbf{Y}_{\{i,l\}}^{j}\right) \end{cases}$$

which implies $\mathbf{Z}_{\{i,l\}}^{j} = \left(\mathscr{P}_{T_{il}} - q_j^{-1} \mathscr{P}_{T_{il}} \mathscr{P}_{\Omega_{il}^{j}} \mathscr{P}_{T_{il}}\right) \left(\mathbf{Z}_{\{i,l\}}^{j-1}\right)$ *and* $\mathscr{P}_{\Omega}\left(\mathcal{Y}\right) = \mathcal{Y}$, *where* $\mathscr{R}\left(\{\mathcal{G}\}\right)$ *means contracting a TR whose singular value matrices are all identity matrices. Note that* $\|\mathbf{Z}_{\{i,l\}}^{j}\|_2 \leq \|\mathscr{P}_{T_{il}} - q_j^{-1} \mathscr{P}_{T_{il}} \mathscr{P}_{\Omega_{il}^{j}} \mathscr{P}_{T_{il}}\|_2 \|\mathbf{Z}_{\{i,l\}}^{j-1}\|_2$, *then*

$$\|\mathscr{P}_{T_{il}}\left(\mathbf{Y}_{\{i,l\}}\right) - \mathcal{U}_{(2)'}^{\{i,l\}} \mathcal{V}_{(2)}^{\{i+l,d-l\}^{\mathrm{T}}}\|_2 = \|\mathbf{Z}_{\{i,l\}}^{j_0}\|_2 \leq 2^{-j_0} \|\mathbf{Z}_{\{i,l\}}^{0}\|_{\mathrm{F}} \leq 2^{-j_0} \sqrt{\underline{n}_{il}} \leq \frac{1}{2} \prod_{i=1}^{d} n_i^{-1}.$$

The proof to the first condition of (6) is complete.

Then we prove the second condition of (6). We deduce

$$
\begin{aligned}
\|\mathscr{P}_{T_{il}^{\perp}}\left(\mathbf{Y}_{\{i,l\}}^{j_0}\right)\|_2 =& \|\sum_{j=1}^{j_0} q_j^{-1}\mathscr{P}_{T_{il}^{\perp}}\mathscr{P}_{\Omega_{il}^{j}}\mathscr{P}_{T_{il}}\left(\mathbf{Z}_{\{i,l\}}^{j-1}\right)\|_2 \\
\leq& \sum_{j=1}^{j_0} q_j^{-1}\|\mathscr{P}_{T_{il}^{\perp}}\mathscr{P}_{\Omega_{il}^{j}}\mathscr{P}_{T_{il}}\left(\mathbf{Z}_{\{i,l\}}^{j-1}\right)\|_2 \\
\leq& \sum_{j=1}^{j_0} \|\left(q_j^{-1}\mathscr{P}_{\Omega_{il}^{j}} - \mathscr{I}\right)\left(\mathbf{Z}_{\{i,l\}}^{j-1}\right)\|_2 \\
\leq& \sum_{j=1}^{j_0} 2C_0\sqrt{q_j^{-1}\overline{n}_{il}\ln\left(\overline{n}_{il}\right)}\|\mathbf{Z}_{\{i,l\}}^{j-1}\|_{\ell_\infty} \\
\leq& \sum_{j=1}^{j_0} 2^{2-j}C_0\sqrt{q_j^{-1}\overline{n}_{il}\ln\left(\overline{n}_{il}\right)}\|\mathbf{Z}_{\{i,l\}}^{0}\|_{\ell_\infty} \\
\leq& 4C_0\sqrt{\frac{\overline{n}_{il}\ln\left(\overline{n}_{il}\right)}{1-(1-p)^{1/j_0}}}\prod_{i=1}^{d}\frac{\mu_{B_i}r_i}{n_i} \\
\leq& 4C_0\sqrt{\frac{j_0\ln\left(\overline{n}_{il}\right)}{m\underline{n}_{il}}}\prod_{i=1}^{d}\mu_{B_i}r_i \\
\leq& 4\sqrt{3}C_0\frac{\log_2\left(\overline{n}_{il}\right)}{\sqrt{m\underline{n}_{il}}}\prod_{i=1}^{d}\mu_{B_i}r_i \\
\leq& \frac{1}{2}.
\end{aligned}
$$

The first inequality comes from the triangle inequality, the second inequality follows form $\mathscr{P}_{T_{il}^{\perp}}\mathscr{P}_{T_{il}} \equiv 0$*, the third inequality is derived by bounding* $\left(q_j^{-1}\mathscr{P}_{\Omega_{il}^{j}} - \mathscr{I}\right)\left(\mathbf{Z}_{\{i,l\}}^{j-1}\right)\|_2$ *using Theorem 6.3 in [31]. The fifth inequality is a result of bounding* $\|\mathbf{Z}_{\{i,l\}}^{0}\|_{\ell_\infty}$ *which can be derived from the proof of Lemma 2. The last inequality requires* C_0 *and* m *are larger enough. The proof to the second condition of (6) is complete.* ■

References

[1] T. G. Kolda, B. W. Bader, Tensor decompositions and applications, SIAM Review 51 (3) (2009) 455–500.

[2] A. Cichocki, D. Mandic, L. De Lathauwer, G. Zhou, Q. Zhao, C. Caiafa, H. A. Phan, Tensor decompositions for signal processing applications: from two-way to multiway component analysis, IEEE Signal Processing Magazine 32 (2) (2015) 145–163.

[3] A. Cichocki, N. Lee, I. Oseledets, A.-H. Phan, Q. Zhao, D. P. Mandic, et al., Tensor networks for dimensionality reduction and large-scale optimization: part 1 low-rank tensor decompositions, Foundations and Trends® in Machine Learning 9 (4-5) (2016) 249–429.

[4] N. D. Sidiropoulos, L. De Lathauwer, X. Fu, K. Huang, E. E. Papalexakis, C. Faloutsos, Tensor decomposition for signal processing and machine learning, IEEE Transactions on Signal Processing 65 (13) (2017) 3551–3582.

[5] M. Signoretto, R. Van de Plas, B. De Moor, J. A. Suykens, Tensor versus matrix completion: a comparison with application to spectral data, IEEE Signal Processing Letters 18 (7) (2011) 403–406.

[6] W. He, L. Yuan, N. Yokoya, Total-variation-regularized tensor ring completion for remote sensing image reconstruction, in: ICASSP 2019-2019 IEEE International Conference on Acoustics, Speech and Signal Processing (ICASSP), IEEE, 2019, pp. 8603–8607.

[7] J. Liu, P. Musialski, P. Wonka, J. Ye, Tensor completion for estimating missing values in visual data, IEEE Transactions on Pattern Analysis and Machine Intelligence 35 (1) (2013) 208–220.

[8] S. Gandy, B. Recht, I. Yamada, Tensor completion and low-n-rank tensor recovery via convex optimization, Inverse Problems 27 (2) (2011) 025010.

[9] C. Mu, B. Huang, J. Wright, D. Goldfarb, Square deal: Lower bounds and improved relaxations for tensor recovery, in: International Conference on Machine Learning, 2014, pp. 73–81.

[10] C. J. Hillar, L.-H. Lim, Most tensor problems are NP-hard, Journal of the ACM 60 (6) (2013) 45.

[11] R. Tomioka, T. Suzuki, K. Hayashi, H. Kashima, Statistical performance of convex tensor decomposition, in: Advances in neural information processing systems, 2011, pp. 972–980.

[12] M. E. Kilmer, K. Braman, N. Hao, R. C. Hoover, Third-order tensors as operators on matrices: a theoretical and computational framework with applications in imaging, SIAM Journal on Matrix Analysis and Applications 34 (1) (2013) 148–172.

[13] Z. Zhang, S. Aeron, Exact tensor completion using t-SVD, IEEE Transactions on Signal Processing 65 (6) (2017) 1511–1526.

[14] J. A. Bengua, H. N. Phien, H. D. Tuan, M. N. Do, Efficient tensor completion for color image and video recovery: low-rank tensor train, IEEE Transactions on Image Processing 26 (5) (2017) 2466–2479.

[15] Y. Liu, Z. Long, C. Zhu, Image completion using low tensor tree rank and total variation minimization, IEEE Transactions on Multimedia 21 (2) (2019) 338–350.

[16] Q. Zhao, M. Sugiyama, A. Cichocki, Learning efficient tensor representations with ring structure networks, arXiv preprint arXiv:1705.08286 (2017).

[17] K. Ye, L.-H. Lim, Tensor network ranks, arXiv preprint arXiv:1801.02662 (2018).

[18] W. Wang, V. Aggarwal, S. Aeron, Efficient low rank tensor ring completion, in: Computer Vision (ICCV), 2017 IEEE International Conference on, IEEE, 2017.

[19] L. Yuan, J. Cao, X. Zhao, Q. Wu, Q. Zhao, Higher-dimension tensor completion via low-rank tensor ring decomposition, in: 2018 Asia-Pacific Signal and Information Processing Association Annual Summit and Conference (APSIPA ASC), IEEE, 2018, pp. 1071–1076.

[20] L. Yuan, C. Li, D. Mandic, J. Cao, Q. Zhao, Tensor ring decomposition with rank minimization on latent space: An efficient approach for tensor completion, in: Proceedings of the AAAI Conference on Artificial Intelligence, Vol. 33, 2019, pp. 9151–9158.

[21] J. Yu, C. Li, Q. Zhao, G. Zhao, Tensor-ring nuclear norm minimization and application for visual: Data completion, in: ICASSP 2019-2019 IEEE International Conference on Acoustics, Speech and Signal Processing (ICASSP), IEEE, 2019, pp. 3142–3146.

[22] H. Huang, Y. Liu, C. Zhu, Provable model for tensor ring completion, arXiv preprint arXiv:1903.03315 (2019).

[23] S. Boyd, N. Parikh, E. Chu, B. Peleato, J. Eckstein, et al., Distributed optimization and statistical learning via the alternating direction method of multipliers, Foundations and Trends® in Machine learning 3 (1) (2011) 1–122.

[24] R. Nishihara, L. Lessard, B. Recht, A. Packard, M. I. Jordan, A general analysis of the convergence of admm, arXiv preprint arXiv:1502.02009 (2015).

[25] C. Lu, A Library of ADMM for Sparse and Low-rank Optimization, National University of Singapore, `https://github.com/canyilu/LibADMM` (June 2016).

[26] Q. Zhao, L. Zhang, A. Cichocki, Bayesian CP factorization of incomplete tensors with automatic rank determination, IEEE Transactions on Pattern Analysis and Machine Intelligence 37 (9) (2015) 1751–1763.

[27] M. F. Barnsley, L. P. Hurd, Fractal image compression, Vol. 1, AK peters Wellesley, 1993.

[28] J. I. Latorre, Image compression and entanglement, arXiv preprint quant-ph/0510031 (2005).

[29] L. Warnke, On the method of typical bounded differences, Combinatorics, Probability and Computing 25 (2) (2016) 269–299.

[30] E. J. Candès, T. Tao, The power of convex relaxation: Near-optimal matrix completion, IEEE Transactions on Information Theory 56 (5) (2010) 2053–2080.

[31] E. J. Candès, B. Recht, Exact matrix completion via convex optimization, Foundations of Computational mathematics 9 (6) (2009) 717.